Acta Crystallographica Section A
Foundations of Crystallography
ISSN 0108-7673

Received 27 August 2009
Accepted 27 October 2009

Low-angle scattering by cylindrical structures

Girija Bhushan Mitra‡

Emeritus Professor, Indian Association for the Cultivation of Science, Jadavpur, Calcutta 700 032, West Bengal, India. Correspondence e-mail: gbmitra@gmail.com

A theory of diffraction at small angles of scattering by a cylindrically constructed structure has been developed and general expressions for two- and three-dimensional cylindrically curved crystallites have been obtained. Modified expressions have been derived for special cases of (*a*) a single arc of equiangularly spaced identical atoms, (*b*) several coaxial arcs each having an equal number of equiangularly spaced identical atoms and (*c*) such arcs arranged at equal distances along the common axis of the arc, including single cylinders and multilayered cylindrical structures. From the expressions obtained, it is possible to measure the magnitudes of the radius of the cylinder, the length of the cylinder, the angular distance between the scattering atoms on each cylindrical arc, their atomic number and the radius of the hole inside each cylindrical structure when a particular tube is considered for a particular purpose or even when predicting the properties required by a nanotube for a particular purpose.

1. Introduction

Recent interest in nanomaterials because of their technical importance has generated enthusiasm for the study of the properties and uses of nanomaterials, including the use of nanotubes and hence of tubular cylindrical structures. The problem of cylindrical structures has been discussed by a number of authors (Fock & Kolpinsky, 1940; Wilson, 1949; Blackman, 1951; Whittaker, 1955; Waser, 1955). The possible types of circular cylindrical lattices have been discussed (Whittaker, 1955), while others (Jagodzinski & Kunze, 1954*a*,*b*,*c*) showed that all cylindrical lattices including spiral and helical structures can be described in terms of radial and axial dislocations. It was shown that all cylindrical lattices can be described in terms of dislocations introduced into a normal three-dimensional lattice of appropriate dimensions (Whittaker, 1955). Fourier transforms of tubular cylindrical objects have also been discussed (Waser, 1955). Cowley (1961) derived expressions for diffraction intensities due to coherently diffracting regions of a crystal in which the lattice is elastically bent. We have earlier described diffraction intensities due to tubular crystals (Mitra, 1965; Mitra & Bhattacherjee, 1968, 1971), and using the formulae derived we studied the structure of metahalloysite (Mitra & Bhattacherjee, 1975). However, very little work seems to have been carried out on the detailed arrangement of atoms in tubular structures or in helical structures.

It is now well known that low-angle-scattering studies often yield direct information regarding the structure of the materials studied because of simplifications in assumptions, such as low-angle scattering by insect flight muscles in rigor (Holmes *et al.*, 1980) and small-angle scattering by helices and random coils in aqueous solutions (Grigoryev *et al.*, 1971). The analytical interpretation of the small-angle X-ray scattering functions for both randomly coiled and helical local conformations of polypeptide chains in solution has been described (Muroga, 2001). Keeping these developments in mind, the present work – to determine the parameters of cylindrical substances by investigations with low-angle scattering assumptions – was undertaken.

2. Theory

2.1. Derivation of an expression for the diffraction intensities due to a cylindrical arrangement of atoms

In Fig. 1, let ABCD represent a layer of identical atoms in the XY plane of a curved crystallite. The repetition of ABCD at regular distance C along the z direction will form the crystallite. In the plane ABCD, the position of an atom P is described by the coordinates ($\mathbf{P}_{mr}$, φ_r), where $\mathbf{P}_{mr} = \mathbf{R} + m\mathbf{b}$ and $\varphi_r = r\varphi$. $|\mathbf{R}|$ is the radius of the first arc AB, $|\mathbf{b}|$ is the radial distance between two successive concentric arcs, φ is the angle subtended at the common center O between two consecutive atoms on the same arc, and m and r are integers including zero. The amplitude of a beam of parallel rays diffracted by this crystallite in the direction $\mathbf{S} = \mathbf{S}_d - \mathbf{S}_0$ ($\mathbf{S}_d$ and $\mathbf{S}_0$ denote unit vectors in the directions of the diffracted and incident beams, respectively) will be proportional to

---

‡ Previously Professor and Head, Department of Physics, Indian Institute of Technology, Kharagput, India. Current address: 284B Rashbehari Avenue, Kolkata 700 019, West Bengal, India.

doi:10.1107/S0108767309044791

$$A(\mathbf{S}) = f(\mathbf{S}) \frac{\sin(\pi/\lambda)T\mathbf{C}\cdot\mathbf{S}}{\sin(\pi/\lambda)\mathbf{C}\cdot\mathbf{S}} \sum_r \sum_m \exp[-(2\pi i/\lambda)(\mathbf{P}_{mr} - \mathbf{P}_0)\cdot\mathbf{S}], \tag{1}$$

where $\mathbf{P}_0$ is the value of $\mathbf{P}$ at the origin, $f(\mathbf{S})$ is the atomic scattering factor of the atom in the direction $\mathbf{S}$, T is the number of layers in the z direction and λ is the wavelength of the diffracted beam. The evaluation of $A(\mathbf{S})$ thus depends upon the evaluation of the quantity $G(\mathbf{S})$ given by

$$G(\mathbf{S}) = \sum_r \sum_m \exp[-(2\pi i/\lambda)(\mathbf{P}_{mr} - \mathbf{P}_0)\cdot\mathbf{S}]. \tag{2a}$$

In other words,

$$\begin{aligned} G(\mathbf{S}) = \sum_r \sum_m \exp\big\{ &-(2\pi i/\lambda)\big[\mathbf{P}_{mr}\cdot\mathbf{S}_d - \mathbf{P}_{mr}\cdot\mathbf{S}_0 \\ &- (\mathbf{P}_0\cdot\mathbf{S}_d - \mathbf{P}_0\cdot\mathbf{S}_0)\big]\big\}. \end{aligned} \tag{2b}$$

Let the incident and diffracted beams make angles α_0 and α with the Y axis as shown in Fig. 1. Let each layer of atoms be composed of M concentric arcs, each arc containing N atoms. Then equation (2a) can be written as (R and b being the dimensions of $\mathbf{R}$ and $\mathbf{b}$, respectively)

$$\begin{aligned} G(\mathbf{S}) &= \sum_{r=0}^{N-1} \sum_{m=0}^{M-1} \exp\Big(-(2\pi i/\lambda)\big\{(R+mb)[\cos(r\varphi+\alpha) \\ &\qquad - \cos(r\varphi+\alpha_0)] - R(\cos\alpha - \cos\alpha_0)\big\}\Big) \qquad (3) \\ &= \exp\{(4\pi i/\lambda)R\sin[(\alpha+\alpha_0)/2]\sin[(\alpha-\alpha_0)/2]\} \\ &\quad \times \sum_{r=0}^{N-1} \sum_{m=0}^{M-1} \exp[(4\pi i/\lambda)(R+mb)\sin(r\varphi+\theta+\alpha_0)\sin\theta], \end{aligned} \tag{4}$$

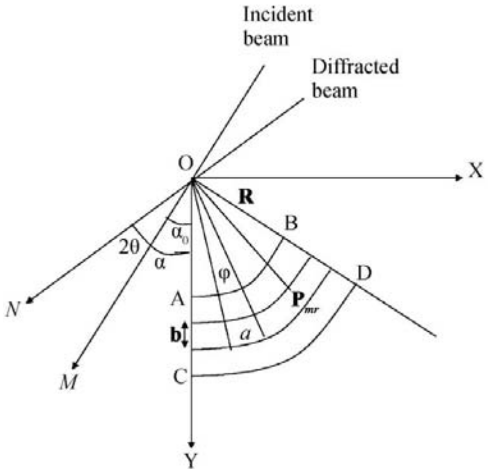

Figure 1
Representation of XY plane of a curved crystallite, where: AOM = α_0 = angle made by incident beam with the Y axis; AON = α = angle made by the diffracted beam with the Y axis; MON = 2θ = the angle of scattering = $\alpha - \alpha_0$; AB = innermost arc; CD = outermost arc; R = radius of the innermost arc; b = radial distance between consecutive arcs; φ = angular separation between two consecutive atoms in the same area; mb = radial distance between two atoms m apart; $r\varphi$ = angular distance between two atoms r apart in the same arc; $\mathbf{P}_{mr}$ = position of the rth atom on the mth arc; a = interatomic distance between two consecutive atoms on the same arc = $R\varphi$; $a_m = (R + mb)\varphi$; C = distance between two consecutive layers in the z direction.

where $\alpha - \alpha_0 = 2\theta$. Therefore

$$\begin{aligned} G(\mathbf{S}) &= \exp\big[(4\pi i/\lambda)R\sin(\theta+\alpha_0)\sin\theta\big] \\ &\quad \times \sum_0^{N-1} \sum_0^{M-1} \exp[(4\pi i/\lambda)(R+mb)\sin(r\varphi+\theta+\alpha_0)\sin\theta]. \end{aligned} \tag{5}$$

Using the relationship (Sneddon, 1956)

$$\exp(ix\sin\psi) = \sum_{p=-\infty}^{\infty} J_p(x)\exp ip\psi$$

with $J_p(x)$ as the pth-order Bessel function of the first kind with argument x, we can write

$$\begin{aligned} G(\mathbf{S}) &= \exp\big[(4\pi i/\lambda)R\sin(\theta+\alpha_0)\sin\theta\big] \\ &\quad \times \sum_{p=-\infty}^{\infty} \sum_0^{N-1} \sum_0^{M-1} J_p[(4\pi/\lambda)\sin\theta(R+mb)] \\ &\quad \times \exp[ip(r\varphi+\theta+\alpha_0)]. \end{aligned} \tag{6}$$

Let us now ignore the z direction and consider a random aggregate of two-dimensional crystals each identical with ABCD and lying in the same plane as ABCD. Then the measured intensity of the beam diffracted in the direction making an angle 2θ with the incident beam will be proportional to the average value of GG^* (where G^* is the complex conjugate of G), the averaging process being carried over all values of α_0 from 0 to 2π at the given value of θ. The measured intensity in the direction of 2θ for such a cluster of two-dimensional curved crystallites will be proportional to

$$\begin{aligned} \langle|GG^*|\rangle &= N^2 \sum_{m=0}^{M-1} J_0^2[(4\pi/\lambda)(R+mb)\sin\theta] \\ &\quad + 2\sum_{p=-\infty}^{+\infty} \sum_{m=0}^{M-1} J_p[(4\pi/\lambda)(R+mb)\sin\theta] \\ &\quad \times \big\{[\sin^2 Np(\varphi/2)]/[\sin^2 p(\varphi/2)]\big\}. \end{aligned} \tag{7}$$

2.2. The two-dimensional crystallite

Equation (7) refers to a two-dimensional crystallite. The third dimension, namely the extension in the z direction, has not been considered here. For a simple circular arc, *i.e.* considering m = 0, the intensity scattered by the crystallite in the angle θ, using equation (7), becomes

$$\begin{aligned} I(\theta) &= N^2 f^2(\theta) J_0^2[(4\pi/\lambda)R\sin\theta] \\ &\quad + 2f^2(\theta) \sum_{p=-\infty}^{+\infty} J_p[(4\pi/\lambda)R\sin\theta] \\ &\quad \times \big\{[\sin^2 Np(\varphi/2)]/[\sin^2 p(\varphi/2)]\big\}, \end{aligned} \tag{8}$$

where $f(\theta)$ is the atomic scattering factor, when the arc comprises N atoms. For a full circle, $N = 2\pi R/a$, where a is the distance along the arc formed between neighboring atoms (see Fig. 1). Thus for a full circle of atoms constituting the crystallite, where p is a positive integer and J_p's with odd values of p will cancel each other, since $J_{-p}(x) = (-1)^p J_p(x)$ (Pierce & Foster, 1957) and $J_p(x) = J_0$ for p = 0,

$$I(\theta) = f^2(\theta)\frac{4\pi^2R^2}{a^2}J_0^2\left(\frac{4\pi R}{\lambda}\sin\theta\right) + 4\sum_{p=+2}^{+\infty} f^2(\theta)J_p\left(\frac{4\pi R}{\lambda}\sin\theta\right)\frac{\sin^2(R/a)p(\varphi/2)}{\sin^2 p(\varphi/2)}. \qquad (9)$$

Assuming N to be of the order of 10, which appears consistent with a nanotube, the first term in equations (7) and (8) will be predominant – particularly because $J_p(x)$ is generally much smaller than $J_0(x)$. The model of equiangularly spaced atoms on a circle or a circular arc sets a limit to the value of φ. The value of N on each coaxial arc is the same. On the arc for which $m = 0$ $N = 2\pi R/a_0$, while for $m = k$ $N = 2\pi[(R + kb)/a_k]$. Thus $a_k - a_0 = 2\pi kb/N$. The interatomic distance a can be stretched only to a certain extent. The value of k will thus depend on the values of N and b. For large R only certain numbers of concentric circles are possible. Thus the model will be of two concentric circles with a permissible thickness. The cases of a solid thick circular cylinder and a circular ring have been solved (Cormack, 1957; Oster & Riley, 1952). However, these authors have assumed a uniform distribution of scattering matter. The current model of an angularly periodical arrangement of point scatterers overcomes the limitations of these cases and provides a wider application, as outlined below.

2.3. The case of cylindrical rods

In actual practice, the cylindrical scatterers may be supposed to consist of several circular rings of point atoms separated by a uniform vertical distance **C**. It has been shown that for an unpolarized primary beam of intensity I_0, the intensity $I(\mathbf{S})$ from a small parallelepipedal crystal is given by (Warren, 1969)

$$I(\mathbf{S}) = I_0 f^2\frac{\sin^2\left[(\pi/\lambda)\mathbf{S}\cdot(N_1\mathbf{A}_1)\right]}{\sin^2\left[(\pi/\lambda)\mathbf{S}\cdot\mathbf{A}_1\right]}\cdot\frac{\sin^2\left[(\pi/\lambda)\mathbf{S}\cdot(N_2\mathbf{A}_2)\right]}{\sin^2\left[(\pi/\lambda)\mathbf{S}\cdot\mathbf{A}_2\right]} \cdot\frac{\sin^2\left[(\pi/\lambda)\mathbf{S}\cdot(N_3\mathbf{A}_3)\right]}{\sin^2\left[(\pi/\lambda)\mathbf{S}\cdot\mathbf{A}_3)\right.}, \qquad (10a)$$

where $\mathbf{S} = \mathbf{S}_d - \mathbf{S}_0$, and $\mathbf{A}_1$, $\mathbf{A}_2$ and $\mathbf{A}_3$ are repeat distances in the x, y and z directions, respectively. Owing to the special cylindrical shape of the scatterers described here, we can take

$$\frac{\sin^2\left[(\pi/\lambda)\mathbf{S}\cdot(N_2\mathbf{A}_2)\right]}{\sin^2\left[(\pi/\lambda)\mathbf{S}\cdot\mathbf{A}_2\right]}\cdot\frac{\sin^2\left[(\pi/\lambda)\mathbf{S}\cdot(N_3\mathbf{A}_3)\right]}{\sin^2\left[(\pi/\lambda)\mathbf{S}\cdot\mathbf{A}_3\right]} = G(\mathbf{S})G(\mathbf{S})^*, \qquad (10b)$$

where $\langle G(\mathbf{S})G(\mathbf{S})^*\rangle$ is the same as in equation (7). The thickness of the cylinder will then be TC if there are T such rings to make up the cylinder, where $T = N_3|\mathbf{A}_3|$ in the equation above, and C is the dimension of **C**. Then the intensity of the scattered radiation is proportional to

$$I(\mathbf{S}) = f^2(\mathbf{S})\langle G(\mathbf{S})G(\mathbf{S})^*\rangle\frac{\sin^2\pi T\mathbf{C}\cdot\mathbf{S}}{\sin^2\pi\mathbf{C}\cdot\mathbf{S}}. \qquad (10c)$$

For a full circular cylinder $N = 2\pi R/a$. For a fragmented cylinder N will depend upon the degree of fragmentation.

2.4. Low-angle approximation

When the angle of scattering θ is low, that is $\theta \to 0$, $\sin\theta \to \theta$. This approximation is valid approximately up to $\theta \to 4°$. Under these conditions

$$\begin{aligned} J_0[(4\pi R/\lambda)\sin\theta] &= J_0(4\pi R\theta/\lambda) \\ &= 1 - \frac{(4\pi\theta/\lambda)^2R^2}{4} + \frac{(4\pi\theta/\lambda)^4R^4}{64} \\ &= 1 - (4\pi^2/\lambda^2)R^2\theta^2 + (4\pi^4/\lambda^4)R^4\theta^4 \end{aligned} \qquad (11a)$$

and

$$\begin{aligned} J_p[(4\pi R/\lambda)\sin\theta] &= J_p(4\pi R\theta/\lambda) \\ &= \frac{(4\pi\theta/\lambda)^pR^p}{2^pP!}\left[1 - \frac{(4\pi\theta/\lambda)^2R^2}{2(p+1)} + \frac{(4\pi\theta/\lambda)^4R^4}{24(2p+2)}\right]. \end{aligned} \qquad (11b)$$

Also, knowing that when p is an integer, $J_{-p}(x) = (-1)^pJ_p(x)$ (Pierce & Foster, 1957), equation (7) becomes

$$\begin{aligned} I(\theta) = {} & N^2f^2(\theta)\sum_{m=0}^{M-1}J_0^2[(4\pi/\lambda)(R+mb)\sin\theta] \\ & + 4f^2(\theta)\sum_{p=1}^{\infty}\sum_{m=0}^{M-1}J_p[(4\pi/\lambda)(R+mb)\sin\theta]\frac{\sin^2 Np(\theta/2)}{\sin^2 p(\theta/2)}. \end{aligned} \qquad (12)$$

Since J_p's with odd values of p will cancel each other, we may accept, according to the first approximation and equation (11),

$$\begin{aligned} I(\theta) &= N^2f^2(\theta)\sum_{m=0}^{M-1}J_0^2[(4\pi/\lambda)(R+mb)\sin\theta] \\ &= N^2f^2(\theta)\sum_{m=0}^{M-1}J_0^2[(4\pi/\lambda)(R+mb)\sin\theta] \\ &= N^2f^2(\theta)\big\{M - (8\pi^2\theta^2/\lambda^2)[MR^2 + 2(M-1)Rb \\ &\quad + (M-1)b^2] + (8\pi^4\theta^4/\lambda^4)[MR^4 + 4(M-1)R^3b \\ &\quad + 6(M-1)R^2b^2 + 4(M-1)Rb^3]\big\}. \end{aligned} \qquad (13)$$

In the first approximation, let us consider $m = 0$ so that the solid rod has only radius R and $N = 2\pi R/a$, and in the low-angle approximation $|S| = (2\pi/\lambda)\sin\theta = 2\pi\theta/\lambda$. Combining equations (7) and (10) we have

$$I(\theta) = f^2(\theta)\langle|GG^*|\rangle\frac{\sin^2\pi T\mathbf{C}\cdot\mathbf{S}}{\sin^2\pi\mathbf{C}\cdot\mathbf{S}}.$$

Taking the first term of equation (7), since $J_0^2(x) \gg J_p(x)$,

$$I(\theta) = f^2(\theta)N^2J_0^2[(4\pi R/\lambda)\sin\theta]\frac{\sin^2(2\pi/\lambda)TC\sin\theta}{\sin^2(2\pi/\lambda)C\sin\theta}. \qquad (14)$$

Now, because of the low-angle approximation, $\sin\theta \to \theta$, therefore

$$I(\theta) = f^2(\theta)N^2J_0^2(4\pi R\theta/\lambda)\frac{\sin^2(2\pi/\lambda)TC\theta}{\sin^2(2\pi/\lambda)C\theta}. \qquad (15)$$

Substituting for N as in equation (9),

$$I(\theta) = \frac{4\pi^2 R^2}{a^2} f^2(\theta) J_0^2\left(\frac{4\pi}{\lambda} R\theta\right) \frac{\sin^2(2\pi/\lambda)TC\theta}{\sin^2(2\pi/\lambda)C\theta}. \tag{16}$$

Then according to equation (11) and the relation $[\sin^2(1/2)nx]/[2\sin^2(1/2)x] = (n/2) + (n-1)\cos x$ [see equation 640 of Pierce & Foster (1957)],

$$\begin{aligned} \frac{\sin^2(1/2)(4\pi/\lambda)TC\theta}{\sin^2(1/2)(4\pi/\lambda)C\theta} &= 2[(T/2) + (T-1)\cos(4\pi/\lambda)C\theta] \\ &= 2[(T/2) + (T-1)], \end{aligned} \tag{17}$$

where $\theta = 0$ and so $\cos(2\pi/\lambda)C\theta = 1$.

Now, when $\theta = 0$, $f(\theta) = Z$, where Z is the atomic number. Also, since $J_0(x) = 1 - (x^2/4) = \exp(-x^2/4)$, so

$$J_0(4\pi R\theta/\lambda) = \exp(-16\pi^2 R^2\theta^2/4\lambda^2) = \exp(-4\pi^2 R^2\theta^2/\lambda^2). \tag{18}$$

Combining equations (17) and (18) and applying them to equation (15), we can write

$$I(\theta) = (4\pi^2 R^2/a^2) Z^2 (3T-2) \exp[-(8\pi^2/\lambda^2) R^2\theta^2] \tag{19}$$

or

$$\ln I(\theta) = 2\ln\left[(2\pi R/a) Z (3T-2)^{1/2}\right] - (8\pi^2/\lambda^2) R^2\theta^2 \tag{20}$$

$$= 2[\ln(2\pi R) + \ln Z - \ln a] + \ln(3T-2) - (8\pi^2/\lambda^2) R^2\theta^2. \tag{21}$$

By taking four readings of $I(\theta)$ at four different values of θ, by changing λ if necessary, for the same tubule, and by applying equation (21), values of R, a, Z and T – the components of the measurements of the tubule – can be determined.

2.5. Application of the results of equations (19) and (21)

The expressions derived in equations (19) and (21) have been applied to the case of a reasonable set of data for an aluminosilicate tubule with an ordinary X-ray source. The assumed values are: $R = 200$ a.u., $a = 4$ a.u., $Z = 4$, $T = 14$, $\lambda = 2$ a.u. For these data, the intensity scattered at the small angle θ according to equation (19) will be

$$\ln I(\theta) = 19.4841 - 8 \times 10^{-5}\theta^2 \tag{22}$$

for $\theta = 0$ to 4°, that is $\theta = 0$ to 0.069 rad.

These values are highly plausible, signifying that the theory and the assumptions made in this work are correct. Equation (22) resembles the well known Guinier equation for scattering at low angles by cylindrical rods (Matsushima *et al.*, 1998).

3. Discussion

Many new materials are based on nanostructured media and have specific properties which strongly depend upon supramolecular organization. One of the uses of nanotubes is for the entrapment of drugs, medicine, proteins, genetic materials *etc*. The clay mineral halloysite is used for this purpose. Recently, the anti-inflammatory agent 5-aminosalicylic acid has been entrapped in tubes of halloysite. Halloysite [$Al_2Si_2O_5(OH)_4$] is a clay mineral of tubular structure (Brindley *et al.*, 1946), which we have earlier shown to have a cylindrical structure (Mitra & Bhattacherjee, 1975). Hollow tubes of halloysite have been studied by Viseras *et al.* (2008) to determine to what extent 5-aminosalicylic acid could be retained by halloysite tubes. By using various techniques they found that aminosalicylic acid molecules are effectively entrapped by halloysite tubes.

Another mineral, imogolite [$AlSiO_3(OH)_4$], should also be mentioned in this connection. It is an important constituent of some types of soils which play important roles in controlling water quality in forest soils and also in other applications. The structure of imogolite has been reported (Cradwick *et al.*, 1972) on the basis of electron-diffraction studies. It consists of aluminosilicate tubes with external diameter 2.1 nm, the tube walls being composed of a di-octahedral gibbsite-like $Al(OH)_3$ sheet with $SiO_2(OH)$ tetrahedra attached to the sheet around the empty octahedral sites. A cross section of an imogolite nanotube described by Pohl *et al.* (1996) is similar to the case shown in Fig. 1, with the first arc belonging to H ($Z = 1$), the next to O ($Z = 8$) followed by Si ($Z = 13$), then Al ($Z = 14$). Hence, in this case, with Al and Si considered approximately the same and contributions from H and O being negligibly small, Fig. 1 can be represented as an equiatomic structure.

Nanotubes of serpentine from the Mighei and Murchison chondrite meteorites are usually 20–230 nm in length and 2–9 nm internal diameter. Owing to their large surface area and hollow structures, they are considered to have served as containers of primordial fluid (Zega *et al.*, 2004). There are many more examples. New types of nanotubes for other purposes can be identified by studying various cylindrical structures by the methods outlined in the equations above. It may be mentioned that the use of equations (19) and (21) enables the user to identify the physical parameters, namely radius and length, of the cylindrical tubule under study and also the chemical nature (Z) and the length constant, a, of the material, assuming it to be 'cylindrical cubic' [extension of orthorhombic (Whittaker, 1955)]. Extensions of equations (19), (20) and (21) by using equations (11), (12) and (13) will enable one to extend the study to the case of multiwalled tubular cylinders. Thus, the parameters of cylindrical structures, such as fiber particles and nanotubes, can be determined.

References

Blackman, M. (1951). *Proc. Phys. Soc. B*, **64**, 625–630.

Brindley, G. W., Robinson, K. & MacEwan, D. M. C. (1946). *Nature (London)*, **157**, 225–226.

Cormack, A. M. (1957). *Acta Cryst.* **10**, 354–358.

Cowley, J. M. (1961). *Acta Cryst.* **14**, 920–927.

Cradwick, P. D. G., Farmer, V. C., Russell, J. D., Masson, C. R., Wada, K. & Yoshinaga, N. (1972). *Nature Phys. Sci.* **240**, 187–189.

Fock, V. A. & Kolpinsky, V. A. (1940). *J. Phys. USSR*, **3**, 125–140.

Grigoryev, A. I., Volkova, L. A. & Ptitsyn, O. B. (1971). *FEBS Lett.* **14**, 189–191.

Holmes, K. C., Tregear, R. T. & Barrington-Leigh, J. (1980). *Proc. R. Soc. London Ser. B*, **207**, 13–33.

Jagodzinski, H. & Kunze, G. (1954*a*). *Neues Jahrb. Mineral. Monatsh.* **6**, 113–130.

Jagodzinski, H. & Kunze, G. (1954*b*). *Neues Jahrb. Mineral. Monatsh.* **7**, 137–150.

Jagodzinski, H. & Kunze, G. (1954*c*). *Neues Jahrb. Mineral. Monatsh.* **10**, 219–240.

Matsushima, N., Izumi, Y. & Aoba, T. (1998). *J. Biochem.* **123**, 150–156.

Mitra, G. B. (1965). *Acta Cryst.* **18**, 464–467.

Mitra, G. B. & Bhattacherjee, S. (1968). *Acta Cryst.* A**24**, 266–269.

Mitra, G. B. & Bhattacherjee, S. (1971). *Acta Cryst.* A**27**, 22–28.

Mitra, G. B. & Bhattacherjee, S. (1975). *Acta Cryst.* B**31**, 2851–2857.

Muroga, Y. (2001). *Biopolymers*, **59**, 320–329.

Oster, G. & Riley, D. P. (1952). *Acta Cryst.* **5**, 272–276.

Pierce, B. O. & Foster, R. M. (1957). *A Short Table of Integrals*, 4th ed. Boston: Ginn and Company.

Pohl, P. I., Faulon, J.-L. & Smith, D. M. (1996). *Langmuir*, **12**, 4463–4468.

Sneddon, I. N. (1956). *Special Functions of Mathematical Physics and Chemistry*, 1st ed. Edinburgh, London: Oliver and Boyd.

Viseras, M. T., Aguzzi, C., Cerezo, P., Cultrone, G. & Viseras, C. (2008). *J. Microencapsul.* pp. 1–8.

Warren, B. E. (1969). *X-ray Diffraction*. Reading: Addison-Wesley Publishing Co.

Waser, J. (1955). *Acta Cryst.* **8**, 142–150.

Whittaker, E. J. W. (1955). *Acta Cryst.* **8**, 571–574.

Wilson, A. J. C. (1949). *Acta Cryst.* **2**, 220–222.

Zega, T. J., Garvie, L. A. J., Dodony, I. & Buseck, P. R. (2004). *Earth Planet. Sci. Lett.* **223**, 141–146.